E17-2002-158

I. V. Barashenkov, S. R. Woodford*, E. V. Zemlyanaya

PARAMETRICALLY DRIVEN DARK SOLITONS

Submitted to «Physical Review Letters»

*Department of Applied Mathematics, University of Cape Town, Rondebosch 7701, South Africa

The parametric driving is well known to be an efficient way of compensating dissipative losses of solitons in various media. Examples include surface solitons in vertically oscillating layers of water [1, 2]; light pulses in optical fibers under phase-sensitive amplification [3] and in Kerr-type optical parametric oscillators [4]; magnetisation solitons in easy-plane ferromagnets exposed to oscillatory magnetic fields in the easy plane [5]. A serious problem associated with the parametric energy pumping, however, is that the driven solitons are prone to oscillatory instabilities which set in as the driver's strength exceeds a certain — often rather low — threshold [6].

With a few notable exceptions, the parametrically driven solitons considered so far had the form of pulses decaying to zero at spatial infinities. These were solutions of the nonlinear Schrödinger (NLS) equation with the "self-focusing"nonlinearity:

$$i\psi_t + \psi_{xx} + 2|\psi|^2\psi - \psi = h\overline{\psi} - i\gamma\psi. \tag{1}$$

(Eq.(1) governs the amplitude of an almost-harmonic stationary wave oscillating with half the frequency of the driver.) However, in a number of applications the amplitude equation of the parametrically driven wave turns out to have the nonlinearity of the "defocusing"type:

$$i\psi_t + \tfrac{1}{2}\psi_{xx} - |\psi|^2\psi + \psi = h\overline{\psi} - i\gamma\psi. \tag{2}$$

The localised solutions forming in the defocusing media are domain walls, or kinks, also known as "dark solitons"in the context of nonlinear optics. The purpose of this note is to explore the stability and bifurcations of the parametrically driven kinks and their bound states.

In fluid dynamics, the "defocusing"parametrically driven NLS (2) describes the amplitude of the oscillation of the water surface in a vibrated channel with large width-to depth ratio [2, 7]. (On the contrary, the "focusing"equation (1) pertains to the case of the narrow channels.) The same equation (2) arises as an amplitude equation for the upper cutoff mode in the parametrically driven damped nonlinear lattices [8]. In the optical context, it was derived for the doubly resonant $\chi^{(2)}$ optical parametric oscillator in the limit of large second-harmonic detuning [9]. Next, in the absence of damping, stationary

solutions $\psi = M_y + iM_z$ of eq.(2) minimise the Ginzburg-Landau free energy for the anisotropic XY model, $F = \int \mathcal{F} dx$, where

$$\mathcal{F} = \tfrac{1}{2}(\partial_x \mathbf{M})^2 - (1+h)\mathbf{M}^2 + \tfrac{1}{2}\mathbf{M}^4 + 2hM_y^2 + \mathcal{F}_0,$$

and $\mathbf{M} = (0, M_y, M_z)$. This model was used to study domain walls in easy-axis ferromagnets near the Curie point [10]. Nonstationary magnetisation configurations were considered in the overdamped limit: $\psi_t = -\delta F/\delta\overline{\psi}$ [11]. The damped hamiltonian dynamics $\psi_t = -i\delta F/\delta\overline{\psi} - \gamma\psi$ provides a sensible alternative; this is precisely our eq.(2).

Before proceeding to its solutions, we show that for $\gamma = 0$ equation (2) has yet another magnetic interpretation. Consider a quasi-one-dimensional ferromagnet with a weakly anisotropic easy plane (M_x, M_y), in the external stationary magnetic field along M_z. The magnetisation vector $\mathbf{M} = (M_x, M_y, M_z)$ lies on the sphere, $\mathbf{M}^2 = M_0^2$, and satisfies the (damped) Landau-Lifshitz equation [12]:

$$\frac{\hbar}{2\mu_0}\mathbf{M}_\tau = \mathbf{M} \times \frac{\delta}{\delta \mathbf{M}} \int \mathcal{W}\, d\xi - \lambda \mathbf{M} \times \mathbf{M}_\tau, \tag{3}$$

$$\mathcal{W} = \frac{\alpha}{2}(\partial_\xi \mathbf{M})^2 + \frac{\beta}{2}M_z^2 + \frac{\epsilon\beta}{2}M_x^2 - HM_z + \mathcal{W}_0. \tag{4}$$

If the anisotropy parameter ϵ is small and the field H is close to βM_0: $H = \beta M_0 - \epsilon q$, the vector $\mathbf{M}$ will stay close to the northern pole of the sphere. We assume $q > \beta M_0/2$ and let

$$M_x + iM_y = (2\epsilon/\beta)^{1/2} s\overline{\psi}$$

with

$$s^2 = qM_0 - \beta M_0^2/2.$$

Assuming that the relaxation constant λ is $\mathcal{O}(\epsilon^{1/2})$ or smaller, and that $\mathbf{M}$ depends only on "slow"variables $x = (\epsilon s^2/2\alpha M_0^2)^{1/2}\xi$ and $t = (2\epsilon\mu_0 s^2/\hbar M_0)\tau$, eq.(3)-(4) reduces to eq.(2) with $h = \beta M_0^2/(2s^2)$ and $\gamma = 0$. Note that the resulting NLS equation is undamped — although the original Landau-Lifshitz equation did include a small damping term.

Solutions of eq.(2) with nonvanishing asymptotics approach, as $|x| \to \infty$, the flat solution $\psi^{(0)} = Ae^{-i\theta}$, where

$$A = (1 + \sqrt{h^2 - \gamma^2})^{1/2}, \quad \theta = \tfrac{\pi}{2} - \tfrac{1}{2}\arcsin(\gamma/h). \tag{5}$$

This flat solution is stable for all $h \geq \gamma \geq 0$. One nonhomogeneous solution is also available in literature [2, 7, 9]:

$$\psi_N(x) = A \tanh(Ax) e^{-i\theta}. \tag{6}$$

For reasons explained below we call it the Néel wall. Our first goal here is to demonstrate a remarkable stability of the Néel wall. We let

$$\psi(x,t) = \psi_N(x) + \delta\psi(x,t),$$

where

$$\delta\psi(x,t) = [u(X) + iv(X)] e^{(\mu-\Gamma)T - i\theta}; \tag{7}$$

$X = Ax$, $T = A^2 t$, $\Gamma = A^{-2}\gamma$ and μ is complex. Linearising eq.(2) in small $\delta\psi$ we obtain an eigenvalue problem

$$(L_0 + \epsilon)v = (\mu - \Gamma)u, \quad L_1 u = -(\mu + \Gamma)v, \tag{8}$$

where $\epsilon = 2 - 2/A^2$ and L_0 and L_1 are the Schrödinger operators with familiar spectral properties:

$$L_0 \equiv -\tfrac{1}{2}\partial_X^2 - \operatorname{sech}^2 X, \quad L_1 \equiv L_0 + 2\tanh^2 X.$$

Introducing $\nu^2 = \mu^2 - \Gamma^2$ and $w = \nu^{-1}(\mu + \Gamma)v$, we eliminate Γ from the eigenvalue problem (8):

$$(L_0 + \epsilon)w = \nu u, \quad L_1 u = -\nu w. \tag{9}$$

Now we will show that $\nu^2 < 0$ for all $0 \leq \epsilon < 2$, so that $\mu^2 < \Gamma^2$ and all perturbations decay to zero as $t \to \infty$.

The operator L_1 has a zero eigenvalue, with the associated eigenfunction $y_0(X) = \operatorname{sech} X$, and no negative eigenvalues. Consequently, on the subspace $\mathcal{R}$ defined by

$$\int u(X) y_0(X) dX = 0, \tag{10}$$

there exists an inverse operator L_1^{-1} and so (9) becomes

$$(L_0 + \epsilon)u = -\nu^2 L_1^{-1} u,$$

with $L_0 + \epsilon$ symmetric and L_1^{-1} a positive operator. The smallest eigenvalue $-\nu_0^2$ is given by the minimum of the Rayleigh quotient:

$$-\nu_0^2 = \min_{u \in \mathcal{R}} \frac{\int u(L_0 + \epsilon) u dX}{\int u L_1^{-1} u dX}. \tag{11}$$

To prove that $-\nu_0^2 > 0$ it is sufficient to show that the minimum of the quadratic form $\int u(L_0 + \epsilon) u dX$ is positive on $\mathcal{R}$ [13]. Assuming that $u(X)$ are normalised by $\int u^2 dX = 1$, the minimum is attained on the solution $u(X)$ to the nonhomogeneous boundary-value problem

$$(L_0 + \epsilon) u(X) = \eta u(X) + \alpha y_0(X), \tag{12}$$

where η and α are the Lagrange multipliers. The minimum equals η — provided η and α are chosen so that the $u(X)$ satisfies eq.(10) and the normalization constraint.

The operator L_0 has a single discrete eigenvalue $E_0 = -\frac{1}{2}$ with the eigenfunction $z_0(X) = (1/\sqrt{2})\mathrm{sech} X$, and the continuous spectrum of eigenvalues $E(k) = k^2$, with

$$z_k(X) = \frac{ik + \tanh X}{ik - 1} e^{-ikx}, \quad -\infty < k < \infty. \tag{13}$$

Expanding y_0 and u over the complete set $\{z_0; z_k\}$ gives

$$y_0(X) = Y_0 z_0(X) + \int Y(k) z_k(X) dk,$$

$$u(X) = U_0 z_0(X) + \int U(k) z_k(X) dk.$$

Substituting into (12) and using the orthogonality of the functions in the set produces $U(k) = \alpha(k^2 + \epsilon - \eta)^{-1} Y(k)$ and $U_0 = \alpha(E_0 + \epsilon - \eta)^{-1} Y_0$. Using these in (10) gives

$$\mathcal{G}_\epsilon(\eta) \equiv \frac{Y_0^2}{E_0 + \epsilon - \eta} + \int_{-\infty}^{\infty} \frac{|Y(k)|^2}{k^2 + \epsilon - \eta} dk = 0. \tag{14}$$

The minimum of the quadratic form $\int u(L_0 + \epsilon) u dX$ is given by the smallest root η^* of the function (14). The function $\mathcal{G}_\epsilon(\eta)$ is increasing for $-\infty < \eta \leq \epsilon$, apart from the point $\eta = E_0 + \epsilon$ where it drops from

$+\infty$ to $-\infty$. As $\eta \to -\infty$, $\mathcal{G}_\epsilon(\eta) \to +0$; as $\eta \to \epsilon$, $\mathcal{G}_\epsilon(\eta)$ tends to a finite value. (This follows from the fact that

$$Y(k) = \frac{ik}{1+ik}\,\frac{\pi k/2}{\sinh(\pi k/2)},$$

hence the integral in (14) converges for all $\eta \leq \epsilon$.) Consequently, there is only one root η^* and its sign is opposite to the sign of $\mathcal{G}_\epsilon(0)$. Since $\partial\mathcal{G}_\epsilon(\eta)/\partial\epsilon < 0$, we have $\mathcal{G}_\epsilon(0) < \mathcal{G}_0(0)$ while the value $\mathcal{G}_0(0)$ can be calculated as

$$\mathcal{G}_0(0) = \frac{Y_0^2}{E_0} + \int_{-\infty}^{\infty} \frac{|Y(k)|^2}{k^2} dk = \int y_0 L_0^{-1} y_0 dX. \qquad (15)$$

Noticing that $L_0^{-1} y_0(X) = -1 + c\tanh X$, with c an arbitrary constant, eq.(15) yields $\mathcal{G}_0(0) = -2$ and hence η^* cannot be negative for any ϵ. Thus $-\nu^2 > 0$ and the Néel wall is stable for all h and γ (with $h \geq \gamma \geq 0$).

We now turn to other solutions of eq.(2), both quiescent and travelling, of the form $\psi(x - Vt)$. We examined their stability numerically, by computing eigenvalues of

$$\mathcal{H}\vec{\varphi} = \lambda J\vec{\varphi}, \qquad (16)$$

where the column $\vec{\varphi} = (u, v)^T$; the operator

$$\mathcal{H} = -\frac{I}{2}\partial_x^2 + \begin{pmatrix} 3\mathcal{R}^2 + \mathcal{I}^2 + h & 2\mathcal{R}\mathcal{I} - V\partial_x + \gamma \\ 2\mathcal{R}\mathcal{I} + V\partial_x - \gamma & \mathcal{R}^2 + 3\mathcal{I}^2 - h \end{pmatrix};$$

and J is an antisymmetric matrix with $J_{21} = -J_{12} = 1$. Eq.(16) is obtained by linearising eq.(2) about $\psi = \mathcal{R} + i\mathcal{I}$ in the co-moving frame, and letting $\delta\psi = (u + iv)e^{\lambda t}$.

Let us start with the undamped situation, $\gamma = 0$, when eq.(2) conserves the energy and momentum integrals:

$$\begin{aligned} E &= \mathrm{Re}\int \left(\frac{|\psi_x|^2}{2} + \frac{|\psi|^4}{2} - |\psi|^2 + h\psi^2 + \frac{|\psi^{(0)}|^4}{2} \right) dx, \\ P &= (i/2)\int (\overline{\psi_x}\psi - \psi_x\overline{\psi}) dx. \end{aligned} \qquad (17)$$

Here eq.(6) coexists with a solution of the form [14]

$$\psi_B(x) = -iA\tanh(2\sqrt{h}x) \pm \sqrt{1-3h}\,\mathrm{sech}(2\sqrt{h}x). \qquad (18)$$

We call it the Bloch wall to emphasise the analogy with Bloch and Néel walls in easy-axis ferromagnets with the second, weaker, anisotropy axis ($\beta, \epsilon < 0$ and $H = 0$ in eq.(4)) [12]. As in that case [12], the energy of our "Bloch wall"is smaller than the energy of the "Néel wall"(6): $E_B = 4\sqrt{h} - \frac{4}{3}h^{3/2}$, $E_N = \frac{4}{3}(1+h)^{3/2}$. (Despite the analogy there are important physical differences; in particular in the easy-axis case the walls interpolate between $\mathbf{M}/M_0 = \pm(0,0,1)$ while in our case they separate domains with $\mathbf{M} \sim (0, \pm\epsilon^{1/2}, 1)$). We have found that the Bloch and Néel walls can travel with nonzero velocity; the travelling solutions are obtained by solving, numerically, the equation

$$\frac{1}{2}\psi_{xx} - iV\psi_x - |\psi|^2\psi + \psi = h\overline{\psi}$$

Similarly to the easy-axis case [12], the distinction between our Bloch and Néel walls becomes less visible as the velocity V grows. Finally, when $V = w$ (an analog of Walker's limit velocity [12]), the two branches merge (Fig.1(a)).

The Bloch wall is known to be the only stable solution of the relativistic and diffusive counterparts of eq.(2) in the region $h < \frac{1}{3}$ where the Bloch and Néel walls coexist. In contrast to those Klein-Gordon and Ginzburg-Landau dynamics [15, 11, 16], our numerical analysis of eq.(16) shows that the entire Bloch-Néel branch of travelling walls in Fig.1(a) is stable. This multistability admits a simple explanation in terms of the energy and momentum, eqs.(17). Since $E_N > E_B$, one might expect ψ_N to decay into ψ_B and radiation waves — as in the relativistic case [15]. However, unlike their relativistic counterparts, our Bloch and Néel walls have unequal momenta, with $P_B > P_N$ (see Fig.1(a)) — and this makes the $\psi_N \to \psi_B$ decay impossible.

Our numerical simulations of eq.(2) showed that two stationary Néel walls repel for $h < \frac{1}{3}$ and attract and annihilate for $h > \frac{1}{3}$. Two stationary Bloch walls of the same chirality (i.e. same sign in (18)) repel whereas walls of opposite chirality attract and form a *nonmoving* stable breather-like state (Fig.1(b)). A stationary Bloch

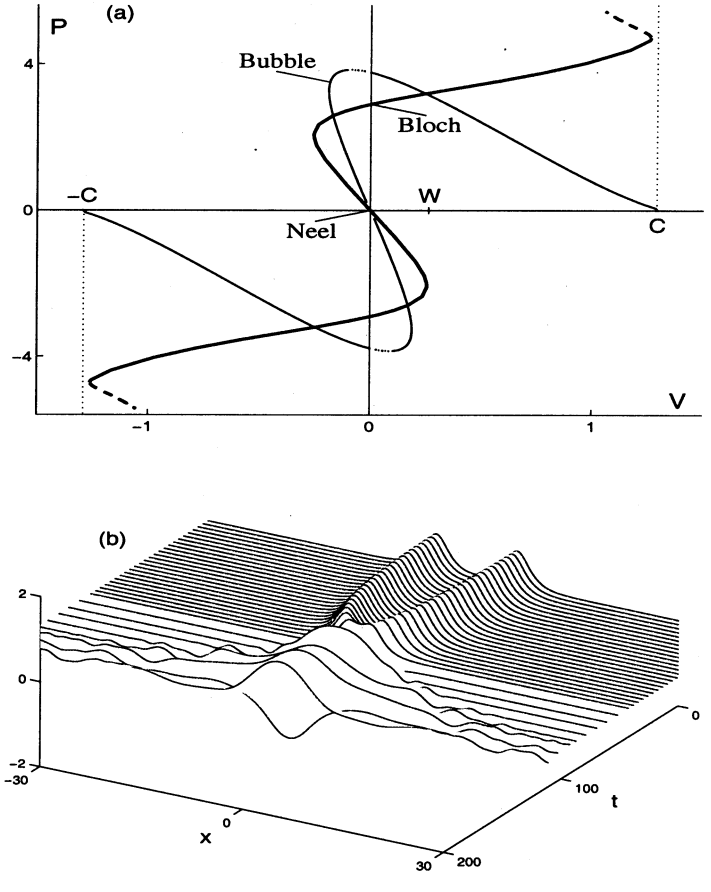

Fig. 1: *(a) The momentum of the travelling Bloch and Néel walls (thick) and their nonoscillatory bubble-like complex (thin line). For $|V|$ close to c, the wall attaches a small-amplitude bubble on each flank; this accounts for the turn of the thick curve near $|V| = c$. The dotted segments of the continuous branches indicate unstable solutions. (b) The formation of an oscillatory breather-like complex of two walls. (Only the real part of ψ is shown for visual clarity.) In (a), $h = \frac{1}{15}$; in (b), $h = 0.1$.*

and Néel wall attract too, which results in a *moving* breather. There also exist nonoscillatory, bubble-like, bound states of the Bloch and Néel wall. (Unlike their parent walls, all of these complexes approach the *same* background as $x \to \infty$ and $x \to -\infty$.) Below we focus on the bubbles and relegate the breathers to a separate publication.

For each h there is a one-parameter family of bubbles, the parameter being the separation distance z between the two walls. (Accordingly, there are two zero eigenvalues in the spectrum of the operator (16) associated with each bubble, one translational and the other one corresponding to variations in z). In this respect the bubble is similar to the complex of two parametrically driven *bright* solitons [17], and like in that case, there is a particular separation $z = \zeta$ for which the bubble is symmetric: $\overline{\psi}_\zeta(-x) = -\psi_\zeta(x)$. For $h = \frac{1}{15}$ we found the analytical form of the symmetric bubble,

$$\psi_\zeta(x) = iA\left[1 - (3/4)\,\mathrm{sech}^2\left(Ax/4 \mp i\pi/4\right)\right]; \qquad (19)$$

for other $h < \frac{1}{3}$ we obtained it numerically. The symmetric bubble turns out to have the largest momentum over bubbles with various z, and ζ is the smallest possible separation: $z \geq \zeta$. The importance of the symmetric bubble stems from the fact that for each h, it is the *only* stable bubble. All nonsymmetric bubbles ($z > \zeta$) were found to have a pair of nonzero, real eigenvalues $\pm\lambda$ in their spectrum. As $z \to \zeta$, the pair converges at the origin and so the symmetric bubble has *four* zero eigenvalues. All other eigenvalues are pure imaginary.

To find the explanation for the stability of the symmetric bubble, we make use of the energy and momentum integrals again. For all h and whatever the separation z, the energy of the bubble ψ_z is *exactly* equal to the sum of the energies of the Bloch and the Néel walls. (For each h and each z the binding energy $E_z - (E_B + E_N)$ was found to be zero to within our computational accuracy, i.e. to within 10^{-10}.) Since for the ($V = 0$)-solutions we have $\delta E = 0$, $\delta^2 E = \int \vec{\varphi}\mathcal{H}\vec{\varphi}dx$, the independence of E of z implies that $\partial_z\vec{\psi} \equiv \partial_z(\mathcal{R}, \mathcal{I})$ is an eigenvector (and not a *generalised* eigenvector) of the operator $\mathcal{H}$ associated with the zero eigenvalue. (In other words, the geometric multiplicity of the zero eigenvalue is two, not one.) Therefore, for small $\epsilon = z - \zeta$, where ζ is the separation corresponding to the bubble with four zero eigenvalues, we have $\mathcal{H}_z = \mathcal{H}_\zeta + \epsilon\mathcal{H}_1 + \ldots$, $\lambda = \epsilon^{1/2}\lambda_1 + \ldots$ and

$Y = Y_0 + \epsilon^{1/2} Y_1 + \ldots$, where Y_0 has to be a linear combination of the two zero modes: $Y_0 = (C_1 \partial_x \vec{\psi} + C_2 \partial_z \vec{\psi})|_{z=\zeta}$. Substituting this into (16), the order $\epsilon^{1/2}$ yields

$$\mathcal{H}_\zeta Y_1 = \lambda_1 J Y_0. \tag{20}$$

Eq.(20) is only solvable if its right-hand side is orthogonal to an independent combination of the two zero modes, i.e. to $C_1 \partial_z \vec{\psi} - C_2 \partial_x \vec{\psi}$. This orthogonality condition amounts to $(dP/dz)|_{z=\zeta} = 0$, and the latter relation explains why the pair of real eigenvalues converges at the origin for the value of z corresponding to the maximum momentum.

The other implication of the relation $dP/dz = 0$ is that it allows the symmetric bubble to be continued to $V \neq 0$ [17]. The resulting branch of moving bubbles is shown in Fig.1(a). As $|V| \to c = \sqrt{1 + 2h + \sqrt{4h(1+h)}}$, which is the minimum phase velocity of linear waves, the bubble degenerates into the flat solution $\psi^{(0)}$, whereas when $V, P \to 0$, the bubble transforms into a pair of Néel walls with the separation $z \to \infty$. The entire branch of moving bubbles is stable, with the exception of a small region between $V = 0$ and the point of the maximum $|P|$ inside which a real pair $\pm\lambda$ occurs (Fig.1(a)). The change of stability at points where $dP/dV = 0$, is explained in [17].

A natural question is which parts of the bifurcation diagram Fig.1(a) persist for nonzero γ. When $\gamma \neq 0$, the energy and momentum are, in general, changing with time:

$$\dot{P} = -2\gamma P, \qquad \dot{E} = \gamma \int (|\psi_0|^4 - |\psi|^4) dx - 2\gamma E,$$

and therefore a steadily travelling soliton has to satisfy

$$P = 0, \qquad E = \frac{1}{2} \int (|\psi_0|^4 - |\psi|^4) dx.$$

In fact, only the first condition needs to be ensured for the continuability. Indeed, for $\psi = \psi(x - Vt)$ eq.(2) with $\gamma = 0$ yields the identity

$$VP = E - (1/2) \int (|\psi_0|^4 - |\psi|^4) dx,$$

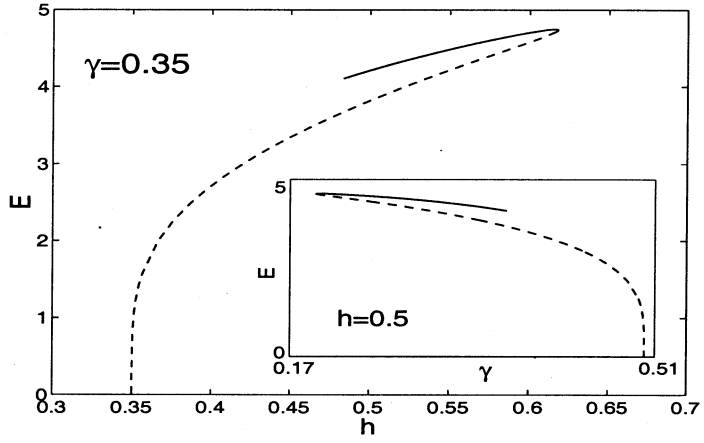

Fig. 2: *The energy of the damped bubble for the fixed γ (main panel) and for the fixed h (inset). The solid and dashed branches indicate stable and unstable solutions, respectively.*

and hence if $P = 0$,

$$E = \frac{1}{2}\int (|\psi_0|^4 - |\psi|^4)dx$$

immediately follows. Since the solid line in Fig.1(a) crosses the $P = 0$ axis only at the stationary Néel wall, we conclude that no other solutions can be continued to small nonzero γ. This does not mean, however, that there are no other solutions for *larger* γ.

Indeed, our simulations revealed a window of h values, $h_1(\gamma) < h < h_2(\gamma)$, where two Néel walls attract and form a stable stationary bubble. Fig.2 shows the energy (17) of the bubble as it is continued in h and γ. (Note that it is *not* continuable to $\gamma = 0$.)

In conclusion, the remarkable stability of the damped-driven kinks and their bound states is in sharp contrast with stability properties of the bright solitons. The stable coexistence of two types of domain walls and their complexes in the undamped case is also worth emphasising; this multistability is not observed in the parametrically driven Klein-Gordon and Ginzburg-Landau equations.

We thank Nora Alexeeva for writing a pseudospectral code for the time-dependent NLS (2) and Boris Ivanov for useful comments

on this work. IB was supported by the NRF and URC grants; SW by the NRF and the Joseph Stone fellowship; EZ by the RFFI grant 000100617.

References

[1] J.W. Miles, J. Fluid Mech. **148**, 451 (1984); W. Zhang and J. Viñals, Phys. Rev. Lett. **74**, 690 (1995); X. Wang and R. Wei, Phys. Rev. **E** 57, 2405 (1998)

[2] C. Elphick and E. Meron, Phys. Rev. A **40**, 3226 (1989)

[3] J.N. Kutz *et al*, Opt. Lett. **18**, 802 (1993)

[4] A. Mecozzi *et al*, Opt. Lett. **19**, 2050 (1994); S. Longhi, Opt. Lett. **20**, 695 (1995); Phys. Rev. **E** 53, 5520 (1996)

[5] I.V. Barashenkov, M.M. Bogdan, and V.I. Korobov, Europhys. Lett. **15**, 113 (1991)

[6] N.V. Alexeeva, I.V. Barashenkov, and D.E. Pelinovsky, Nonlinearity **12**, 103 (1999); V.S. Shchesnovich and I.V. Barashenkov, Physica D **164**, 83 (2002)

[7] B. Denardo *et al*, Phys. Rev. Lett. **64**, 1518 (1990)

[8] B. Denardo *et al*, Phys. Rev. Lett. **68**, 1730 (1992); G. Huang, S.-Y. Lou, and M. Velarde, Int. J. Bif. Chaos **6**, 1775 (1996)

[9] S. Trillo, M. Haelterman and A. Sheppard, Opt. Lett. **22**, 970 (1997)

[10] L.N. Bulaevskii and V.L. Ginzburg, Sov. Phys. JETP, **18**, 530 (1964); J. Lajzerowicz and J.J. Niez, J. de Phys. **40**, L165 (1979)

[11] P. Coullet *et al*, Phys. Rev. Lett. **65**, 1352 (1990); P. Coullet, J. Lega and Y. Pomeau, Europhys. Lett. **15**, 221 (1991); D.V. Skryabin *et al*, Phys. Rev. E **64**, 056618 (2001)

[12] A.M. Kosevich, B.A. Ivanov, and A.S. Kovalev, Phys. Rep. **194**, 117 (1990)

[13] N.G. Vakhitov and A.A Kolokolov, Radiophys. Quantum. Electr. **16** (1975) 783

[14] S. Sarker, S.E. Trullinger and A.R.Bishop, Phys. Lett. A **59** (1976) 255

[15] P. Hawrylak, K.R. Subbaswamy, S.E. Trullinger, Phys. Rev. D **29**, 1154 (1984)

[16] B.A. Ivanov, A.N. Kichizhiev, and Yu.N. Mitsai, Sov. Phys. JETP **75**, 329 (1992)

[17] I.V. Barashenkov, E.V. Zemlyanaya, M. Bär, Phys. Rev. E **64**, 016603 (2001)

Received on July 4, 2002.

Барашенков И. В., Вудфорд С. Р., Земляная Е. В.
E17-2002-158

Темные солитоны с параметрической накачкой

Показано, что в отличие от случая светлых солитонов параметрическая накачка не приводит к неустойчивости доменных стенок (темных солитонов) ни при каких значениях амплитуды накачки и коэффициента диссипации. Показано также, что параметрически возбуждаемые доменные стенки способны образовывать устойчивые связанные состояния. В отсутствие диссипации устойчивые доменные стенки двух типов и их устойчивые связанные состояния способны двигаться с ненулевой скоростью.

Работа выполнена в Лаборатории информационных технологий ОИЯИ.

Препринт Объединенного института ядерных исследований. Дубна, 2002

Barashenkov I. V., Woodford S. R., Zemlyanaya E. V.
E17-2002-158

Parametrically Driven Dark Solitons

We show that unlike the bright solitons, the parametrically driven kinks are immune from instabilities for all dampings and forcing amplitudes; they can also form stable bound states. In the undamped case, the two types of stable kinks and their complexes can travel with nonzero velocities.

The investigation has been performed at the Laboratory of Information Technologies, JINR.

Preprint of the Joint Institute for Nuclear Research. Dubna, 2002

Макет *Т. Е. Попеко*

ЛР № 020579 от 23.06.97.
Подписано в печать 24.07.2002.
Формат 60 × 90/16. Бумага офсетная. Печать офсетная.
Усл. печ. л. 0,93. Уч.-изд. л. 0,96. Тираж 315 экз. Заказ № 53443.

Издательский отдел Объединенного института ядерных исследований
141980, г. Дубна, Московская обл., ул. Жолио-Кюри, 6.